



**HAL**  
open science

## Zr-shift at the origin of the exceptional piezoelectric properties of $\text{PbZr}_{0.52}\text{Ti}_{0.48}\text{O}_3$

Ali Al-Zein, G. Fraysse, Jérôme Rouquette, Ph. Papet, J. Haines, B. Hehlen, C. Levelut, G. Aquilanti, Yves Joly

► **To cite this version:**

Ali Al-Zein, G. Fraysse, Jérôme Rouquette, Ph. Papet, J. Haines, et al.. Zr-shift at the origin of the exceptional piezoelectric properties of  $\text{PbZr}_{0.52}\text{Ti}_{0.48}\text{O}_3$ . *Physical Review B: Condensed Matter and Materials Physics* (1998-2015), 2010, 81 (17), pp.4110. 10.1103/PhysRevB.81.174110. hal-00527699v1

**HAL Id: hal-00527699**

**<https://hal.science/hal-00527699v1>**

Submitted on 20 Oct 2010 (v1), last revised 20 Oct 2010 (v2)

**HAL** is a multi-disciplinary open access archive for the deposit and dissemination of scientific research documents, whether they are published or not. The documents may come from teaching and research institutions in France or abroad, or from public or private research centers.

L'archive ouverte pluridisciplinaire **HAL**, est destinée au dépôt et à la diffusion de documents scientifiques de niveau recherche, publiés ou non, émanant des établissements d'enseignement et de recherche français ou étrangers, des laboratoires publics ou privés.

# Zr-shift at the Origin of the Exceptional Piezoelectric Properties in $\text{PbZr}_{0.52}\text{Ti}_{0.48}\text{O}_3$

A. Al-Zein<sup>1,2</sup>, G. Frayssé<sup>1</sup>, J. Rouquette<sup>1</sup>, Ph. Papet<sup>1</sup>, J. Haines<sup>1</sup>, B. Hehlen<sup>2</sup>, C. Levelut<sup>2</sup>, G. Aquilanti<sup>3</sup>, Y. Joly<sup>4</sup>

<sup>1</sup>*Institut Charles Gerhardt Montpellier, UMR CNRS 5253, équipe C2M, Université Montpellier II, 34095 Montpellier cedex 5, France.*

<sup>2</sup>*Laboratoire des Colloïdes, Verres et Nanomatériaux (LCVN), UMR CNRS 5587, Université Montpellier II, 34095 Montpellier cedex 5, France.*

<sup>3</sup>*European Synchrotron Radiation Facility, 6 rue Jules Horowitz, B.P. 220 38043 Grenoble cedex 09, France. and*

<sup>4</sup>*Institut Néel, CNRS, Université Joseph Fourier, BP166, 38042 Grenoble cedex 9, France.*

In spite of intensive experimental and theoretical studies, no model at the atomic scale has been proposed to explain the large piezoelectric effect in  $\text{PbZr}_{0.52}\text{Ti}_{0.48}\text{O}_3$  (PZT) compared to the low piezoelectric response in the simple end-member lead titanate  $\text{PbTiO}_3$ . X-ray Absorption Spectroscopy (XAS) appears as the technique of choice not only to clarify the role of Zr, but also to quantify the Zr displacement through the Ferroelectric-Paraelectric (*F-P*) transition. We clearly show evidence of the polar character of the Zr-atoms in PZT with a Zr-shift which will produce a small polarization. Such an atomic configuration for one type of atoms leads to relatively easy switching, i.e. relatively low electric field to align the Zr-polar atoms, which will create a favourable energetic situation for the cooperative switching of the strongly polar Ti-O dipole and would therefore account for the large piezoelectric effect in PZT.

Understanding the physical behavior of a material at the atomic scale has always presented a great challenge to condensed matter physicists and materials scientists. The effort to elucidate the role played by Zr/Ti atoms which are at the origin of the polar displacements in ferroelectric  $\text{PbZr}_{0.52}\text{Ti}_{0.48}\text{O}_3$  (PZT) is a prime example of such a challenge [1–3]. PZT exhibits a *F-P* phase transition at a critical temperature  $T_C$  (and a critical pressure  $P_C$ ), which can be defined from a structural point of view as a phase transition from a non-centrosymmetric to a centrosymmetric structure and due to the disappearance of the spontaneous polarization characterizing these materials [4]. The origin of the large dielectric susceptibility and piezoelectric properties in these highly polarizable ferroelectric perovskite of general formula  $\text{ABO}_3$  is due to the cooperative displacement of the *B* cations, i.e. the Zr/Ti atoms in our case, from the center of symmetry of their octahedral sites below a critical temperature  $T_C$  (and critical pressure  $P_C$ ). These spontaneous displacements create local dipoles that are aligned parallel one to another in order to give a macroscopic dipole moment by application of an electric field *E*.

PZT is widely used in technological applications due to its high piezo-ferro electric properties. This particular composition, i.e.  $x = 0.48$  in the  $\text{Pb}(\text{Zr}_{1-x}\text{Ti}_x)\text{O}_3$  solid solution, exhibits the highest electromechanical response and is generally termed as the Morphotropic Phase Boundary (MPB) separating the Zr-rich rhombohedral from the Ti-rich tetragonal phase [5]. In the paraelectric form (above  $T_C = 664$  K), PZT is cubic with a Pb atom at each corner of the cubic lattice, the Ti/Zr atoms in the center and the oxygen atoms are at the centers of the faces. Upon decreasing temperature, both Pb and Ti/Zr will move along the pseudocubic  $[001]_c$  axis giving rise to the tetragonal form. The  $3d^0/4d^0$  state of the Ti/Zr atoms can give an insight to the local shifts on

the same site, i.e. the center of the oxygen octahedron.  $\text{Zr}^{4+}$  and  $\text{Ti}^{4+}$  have ionic radii of 0.72 Å and 0.605 Å respectively [6]. One can therefore expect a much more pronounced off-center shift of smaller Ti-atoms in their oxygen octahedra cage in comparison to the larger Zr-atoms. This scenario was confirmed based on XAS [7] and Pair Distribution Function measurements [8]; the Ti off-center displacement is experimentally found to be about 0.2-0.3 Å, while Zr is found to have either a small shift (0.07 Å) [7] or no shift [8]. Additionally, although the Zr-shift is found to be both temperature and composition independent [7, 9], the Ti-shifts appear to have an order-disorder component as a function of temperature [10] and pressure [11] which was found to be quite unusual for these ferroelectric displacive-type transitions [12]. This Letter provides the evidence of the ferroelectric character of the Zr-atoms in PZT in the *P-T* space. The small Zr-shifts (0.06 Å) are found to disappear with a small order-disorder component above the ferroelectric-paraelectric transition based on i- the behaviour as a function of pressure of the EXAFS Debye-Waller factor (DWF)  $\sigma^2$  which accounts for the disorder in the Zr-O distance and ii- the smooth decrease in intensity of the Pre-edge Fine Structure (PEFS) which is associated with the loss of the dipolar contribution.

Zr *K* edge measurements (17998 eV) at high pressure and 2 isotherms (300 K, 450 K) were performed in Paris-Edinburgh press in transmission geometry at beamline BM29 of the European Synchrotron Radiation Facility. The EXAFS data analysis was carried out with the IFFIT package [13]. The FDMNES code [14] was used for the XANES analysis. The complete experimental procedure can be found in the Electronic Physics Auxiliary Publication Service (EPAPS).

High quality, high-pressure XAS data of PZT were normalized to the jump at the absorption edge and the ap-

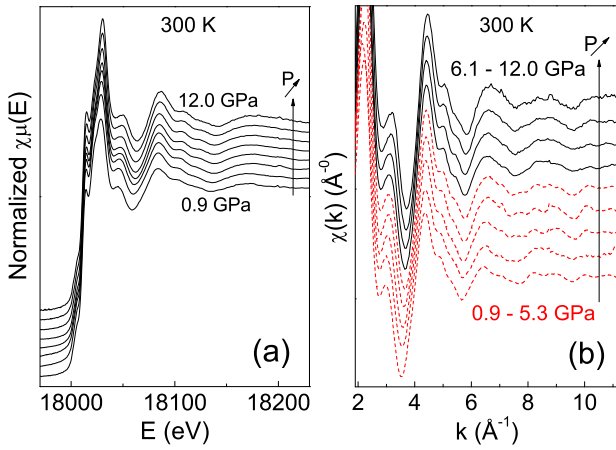


FIG. 1. (color online) a) Normalized XAS spectra obtained at 300 K between 0.9 GPa and 12 GPa, b) Extracted  $\chi(k)$ . Both signals are vertically shifted for clarity.

parent small effect of pressure on the Zr  $K$  edge spectra can be seen, Figure 1a. Namely, the extracted  $\chi(k)$  spectra, Figure 1b, evidence above 6.1 GPa a disappearance of some high frequency contributions: in particular the split doubled features between  $k = 6 \text{ \AA}^{-1}$  and  $k = 7.5 \text{ \AA}^{-1}$  and between  $k = 8 \text{ \AA}^{-1}$  and  $k = 10 \text{ \AA}^{-1}$  merge into two single oscillations respectively. Based on these data, there might be a low pressure behavior below  $\sim 6.1$  GPa, and a high pressure behavior above.

In figure 2a, we show Fourier transforms of the EXAFS signal at 3.7 GPa and 7.0 GPa whose first peak can be correlated to the radial distribution function around the photoabsorber. At 7.0 GPa, the maximum of the peak is shifted with respect to that at 3.7 GPa indicating a weak contraction of the Zr-O distance and the peak amplitude is higher. Nonetheless the shape of the first peak of the Fourier transform is a Gaussian at all pressures allowing us to use the same structural model given by six oxygen atoms as first neighbours at the same distance. The fitting was done in  $q$  space isolating the Zr-O peak of the Fourier transform and the back transforming in  $q$  space using a standard procedure. A symmetric distribution of bond distances was used, characterized by the following structural parameters:  $R$  (average bond distance),  $\sigma^2$  (relative mean square displacement or EXAFS DWF:  $\exp(2\sigma^2 k^2)$ ), and the number of neighbours which was kept fixed to six. Figures 2b and 2c show the Zr-O atom pair distribution function, i.e. backward Fourier transform, in the  $k^3$ -weighted space along with the best fit calculation obtained at 3.7 GPa and 7 GPa. The experimental data are correctly reproduced within the pressure range of investigation.

Figure 2d shows the pressure behavior of the experimental  $\sigma^2$  for the Zr-O atom pairs at 300 K;  $\sigma^2$  accounts for the mean square displacement of the Zr-O distance and contains two contributions: a thermal ( $\sigma_{dyn}^2$ ) and

a structural ( $\sigma_{stat}^2$ ) contribution linked to the local vibrational dynamics and the local structural distortions, respectively. One can first note that the fitted ambient value is perfectly consistent with that reported in the literature [7] (the open star). Additionally, a noticeable decrease of  $\sigma^2$  can be observed with increasing pressure with a change in the trend at  $\sim 7$  GPa.

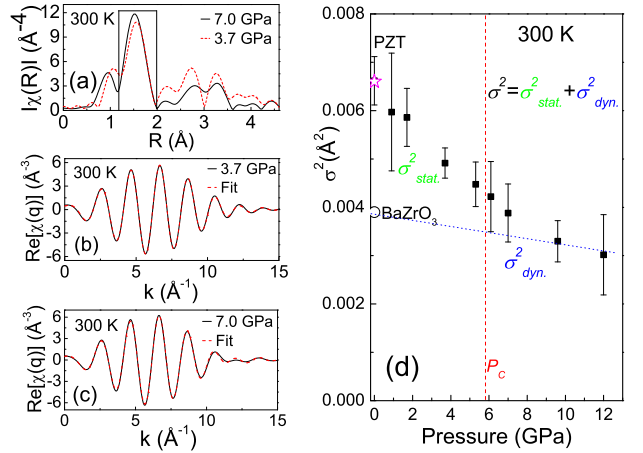


FIG. 2. (color online) a) The  $k^3$ -weighted EXAFS signals (obtained in the  $2\text{-}11 \text{ \AA}^{-1}$  range) are shown at 3.7 GPa (dashed) and 7.0 GPa (full). The Zr-O first coordination shell is extracted using a Hann window in the  $1.2\text{-}2 \text{ \AA}$  range. b) and c) The  $k^3$ -weighted backward Fourier transforms along with the resulting fits (dashed) are shown at 3.7 GPa and 7 GPa respectively. d) Pressure behavior of the DWF for the Zr-O atom pairs at 300 K. Values reported in the literature for PZT [7] (\*) and BaZrO<sub>3</sub> [15] (o) are also included.  $P_C$  (the dashed line) corresponds to the paraelectric transition [18]. The dotted line represents the decrease of  $\sigma_{dyn}^2$  as explained in the text.

To interpret these data, it is important to compare them with the  $\sigma^2$  obtained in BaZrO<sub>3</sub> (BZ) where the Zr atoms are known to be perfectly centrosymmetric (Zr in the centre of the oxygen octahedra) in the whole pressure-temperature range [15], implying that the  $\sigma^2$  in BZ is only dependent on the thermal vibrations ( $\theta_E = 606$  K) and does not contain the static contribution [16]. The behavior of  $\sigma_{dyn}^2$  (BZ) at a fixed temperature (300 K) can be expected to smoothly decrease upon increasing pressure. This decreasing behaviour of  $\sigma_{dyn}^2$  (dotted line in Figure 2d) can be estimated using the equivalent isotropic temperature factors of the  $B$  atom reported in a high pressure single crystal diffraction study [17] of GdFeO<sub>3</sub>, a centrosymmetric perovskite (no static disorder) which exhibits no phase transition in the pressure range of interest. The pressure dependence of  $\sigma_{dyn}^2$  corresponds to a decrease of about 1% per GPa [17]. At ambient conditions, we can observe that the  $\sigma^2$  of PZT is higher than that of BZ, this can be attributed to the presence of static disorder in PZT, which is absent in BZ. At high pressure, the  $\sigma_{dyn}^2$  estimation of BZ perfectly fits the high pressure values of  $\sigma^2$  for PZT indicating that pres-

sure eliminates the static disorder for the Zr-atoms of PZT above 7 GPa and that the only contribution to the EXAFS DWF is dynamic above this pressure. Based on previous studies, we have already characterized the ferroelectric-paraelectric phase transition of PZT at 5-6 GPa [18], Figure 2d ( $P_C$ : dashed line). This phase transition can be linked to the change in the decrease of  $\sigma^2$  for the Zr-O bond and the situation (low pressure regime) in which the EXAFS DWF contains the static and dynamic contributions and that (high pressure regime) in which only the dynamic part contribute to the  $\sigma^2$ . This implies that  $\sigma_{stat}^2$  of PZT is due to a small random Zr off-center displacement in the oxygen octahedra cage, which will produce a small polarization. This Zr-shift can be roughly estimated  $\sim 0.06 \text{ \AA}$ , i.e.  $\sqrt{0.0067 - 0.003} \cong 0.06 \text{ \AA}$ . The excess of  $\sigma_{stat}^2$  appears at pressures well above  $P_C$  suggesting an order-disorder nature of the transition, as it has already been reported for Ti-shifts in  $P$ - $T$  space [10, 11]. It is worth to stress that beside the displacement of Zr from the offset position to the centrosymmetric position of  $0.06 \text{ \AA}$ , the average Zr-O distances contract by  $0.01 \text{ \AA}$  indicating the small compressibility of the oxygen octahedra.

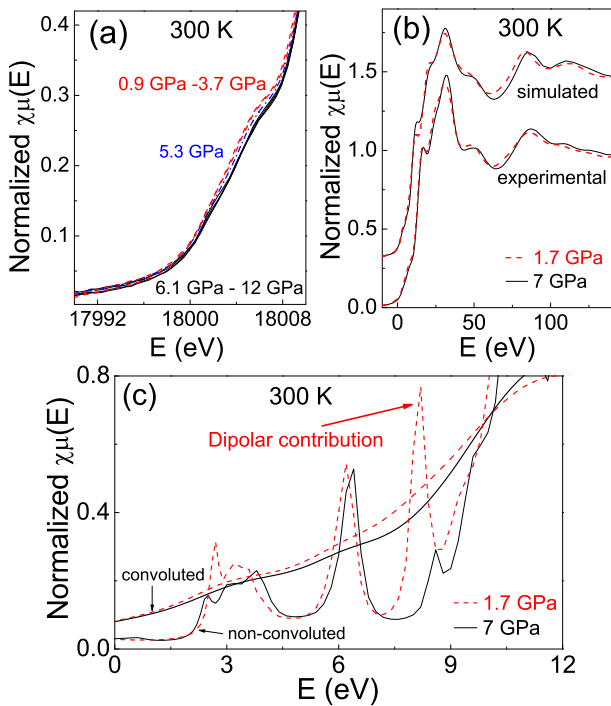


FIG. 3. (color online) a) High-pressure Zr  $K$  edge XANES spectra obtained at 300 K. Note the pressure evolution of the PEFS. b) Experimental and simulated XANES spectra at 1.7 GPa and 7 GPa. In b), the origin (0) corresponds to the Zr  $K$  edge. c) The non-convoluted and convoluted theoretical PEFS at 1.7 GPa and 7 GPa showing the disappearance of the dipolar contribution at high pressure.

Let us now discuss about the XANES part of the spectra. The  $p$ - $d$  peak, linked to the dipole transition, is ex-

pected to disappear at the ferroelectric-paraelectric transition as in  $\text{PbTiO}_3$ . However, it is difficult to observe this effect in PZT [9] at Zr  $K$  edge owing to the large Zr  $K$  hole width ( $\gamma_K(\text{Zr}) \approx 3.84 \text{ eV}$ ) as compared to that of Ti  $K$  edge in  $\text{PbTiO}_3$  ( $\gamma_K(\text{Ti}) \approx 0.8 \text{ eV}$ ). The very weak variation of  $\sigma_{dyn}^2$  in this high-pressure experiment enabled us to distinguish a smooth, but observable decrease in the PEFS intensity in the 0.9 GPa - 6.1 GPa pressure range, as shown in Figure 3a. Above 6.1 GPa, the PEFS spectra overlap almost perfectly. The critical pressure for the change in behavior, i.e. 6.1 GPa, is roughly consistent with the results described above, figures 1b and 2d. In order to determine the origin of the change in the behavior in the XANES spectra, we performed full multiple scattering calculations. Based on our structural data obtained from neutron diffraction [18], an excited atom embedded in a  $10 \text{ \AA}$ -cluster was used to simulate the XANES spectra in the ferroelectric and paraelectric state. In the ferroelectric state, a Zr-displacement of  $0.06 \text{ \AA}$  from the symmetric position was kept fixed consistent with the EXAFS results. The theoretical spectra were convoluted with contributions due to the Zr  $K$  hole width, the photoelectron width and the experimental resolution. Figure 3b shows the experimental and simulated XANES spectra obtained at 1.7 GPa and 7 GPa, which are consistent with a long range polar and non-polar state. All the features are correctly reproduced starting from the more intense white line in the paraelectric state, centred at 30 eV, to the well-known shift to higher energy of the XANES spectrum at high pressure. Note, however, that large convolution with the contribution due to the Zr  $K$  hole width hides the structure at low energy. We show thus in Figure 3c, the non-convoluted (before broadening) and convoluted spectra at 1.7 GPa and 7 GPa. It is here clearly possible to identify the dipolar contribution in the low-pressure spectrum at about 8.2 eV due to the breaking of the inversion symmetry induced by the small Zr-shift from its symmetric position. At high pressure in the paraelectric state, i.e. 7 GPa, only the quadrupolar contribution for which intensities are only very weakly affected by the Zr-shift can be observed. Therefore contrary to what was expected, these simulations confirm that even a small Zr-shift can be observed in the PEFS signal. This confirms that XAS measurements are a perfect probe of local polar displacements. Note that for the EXAFS analysis mentioned above, the small Zr-shift can only be observed due to the high-pressure measurements at constant temperature. As stated previously, the thermal vibrations in our case are almost constant thereby making the interpretation considerably easier.

Figure 4a shows the pressure behavior of the experimental  $\sigma^2$  for the Zr-O atom pairs at 450 K. As observed at ambient temperature, a noticeable decrease of  $\sigma^2$  can be observed with increasing pressure followed by a plateau at higher pressures. The calculated value of  $\sigma^2$

in BZ at 450K is plotted ( $\theta_E = 606$  K) [16]. As in Figure 2d, the  $\sigma_{dyn}^2$  estimation of BZ (dotted line) is inserted and perfectly fits again with the values of  $\sigma^2$  for PZT at high pressure giving an additional evidence that pressure eliminates the static disorder for the Zr-O bond in PZT above 5 GPa; again the only contribution to the EXAFS Debye-Waller factor above this pressure will be dynamic. As observed previously,  $\sigma_{stat}^2$  of PZT comes from a small random Zr off-center displacement in the oxygen octahedron cage which will produce a small polarization. This finding is supported by the high-pressure XANES spectra obtained at 450 K, Figure 4b. It is possible to distinguish a smooth decrease in the PEFS intensity in the 0.9 GPa - 5.7 GPa pressure range. Above 5.7 GPa, the PEFS spectra overlap almost perfectly indicating the disappearance of the dipolar contribution as shown by the full multiple scattering calculations mentioned above.

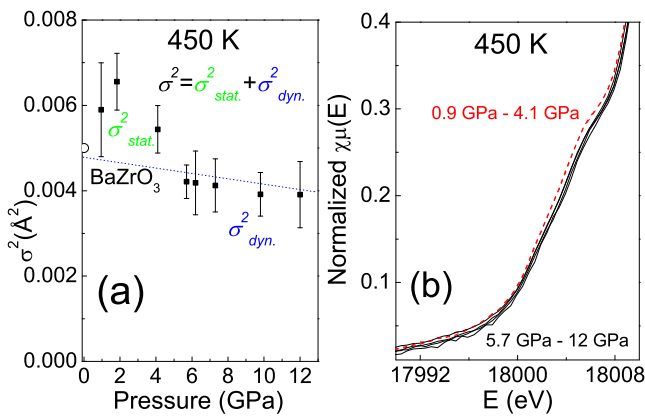


FIG. 4. (color online) a) Pressure behavior of the DWF for the Zr-O atom pairs at 450 K. The calculated value for BaZrO<sub>3</sub> (c) [15] is also included.  $\sigma_{dyn}^2$  (the dotted line) corresponds to a decrease of about 1% per GPa. b) High-pressure Zr *K* edge XANES spectra obtained at 450 K. Note the pressure evolution of the PEFS.

To conclude, this XAS study as a function of pressure and temperature provides the first evidence of the polar character of the Zr-atoms in PZT with a Zr-shift, which will produce a small Zr polarization. This small polarization can therefore be aligned with a modest electric field which would create a favourable energetic situation for the switching of the strongly polar Ti-O dipole and would therefore account for the large piezoelectric effect in PZT. Viewed from the zirconium site, the local configuration is similar to that expected close to  $T_C$  in a classical ABO<sub>3</sub> ferroelectric, at which a maximum in the dielectric constant is observed, i.e. the coercitive electric field necessary to switch the polarisation drastically decrease. In mixed *B*-cation systems, such local configurations for one type of *B*-cations leads to relatively easy switching giving rise to exceptional ferro/piezoelectric properties. It is interesting to note that this MPB composition, which

exhibits the highest piezoelectric performances, has a Zr/Ti compositional ratio of 1/1 which would optimize the process described above. Furthermore, we can analyze other ferroelectric materials, which also present high or giant piezoelectric effect, the PbMg<sub>1/3</sub>Nb<sub>2/3</sub>O<sub>3</sub> and PbZn<sub>1/3</sub>Nb<sub>2/3</sub>O<sub>3</sub> systems for example. Looking at the  $d^0$  state of the Mg/Nb and Zn/Nb atoms, it is possible to predict similar behavior. Here, the strong dipole will be Nb-O with small Nb<sup>5+</sup> of 0.64 Å, while the small polarization will be produced by the larger Mg<sup>2+</sup> or Zn<sup>2+</sup>, 0.72 Å and 0.74 Å respectively [6]. One can clearly expect that the Mg- and Zn- atom could be easily poled with a modest applied electric field like the Zr-atom in our study providing an effective way to align the Nb-O dipoles. Finally, this result could be an interesting way to predict new ferroelectric materials with optimal ferro-piezo-electric properties.

- [1] R. E. Cohen, Nature **358**, 136 (1992).
- [2] I. Grinberg, V. R. Cooper, and A. M. Rappe, Nature **419**, 909 (2002).
- [3] A. M. George, J. Iniguez, and L. Bellaiche, Nature **413**, 54 (2001).
- [4] M. E. Lines, and A. M. Glass, Principles and Applications of Ferroelectrics and Related Materials (Clarendon, Oxford, 1977).
- [5] B. Jaffe, W. R. Cook, and H. Jaffe, Piezoelectric Ceramics (Academic, London, 1971).
- [6] R. D. Shannon, Acta Crystallographica **A32**, 751 (1976).
- [7] D. Cao, I. K. Jeong, R. H. Heffner, T. Darling, J. K. Lee, F. Bridges, J. S. Park, and K. S. Hong, Phys. Rev. B **70**, 224102 (2004).
- [8] W. Dmowski, T. Egami, L. Farber, and P. K. Davies, Fundamental Physics of Ferroelectrics (AIP conference proceedings) **582**, 33 (2001).
- [9] R. V. Vedrinskii, E. S. Nazarenko, M. P. Lemeshko, V. Nassif, O. Proux, A. A. Novakovich, and Y. Joly, Phys. Rev. B **73**, 134109 (2006).
- [10] N. Sicron, B. Ravel, Y. Yacoby, E. A. Stern, F. Dogan, and J. J. Rehr, Phys. Rev. B **50**, 13168 (1994).
- [11] N. Jaouen, A. C. Dhaussy, J. P. Iti, A. Rogalev, S. Marinel, and Y. Joly, Phys. Rev. B **75**, 224102 (2004).
- [12] W. Cochran, Adv. Phys. **10**, 401 (1961).
- [13] M. Newville, J. synchrotron Rad. **8**, 322 (2001).
- [14] Y. Joly, Phys. Rev. B **63**, 125120 (2001).
- [15] C. Laulhe, F. Hippert, J. Kreisel, M. Maglione, A. Simon, J. L. Hazemann, and V. Nassif, Phys. Rev. B **74**, 014106 (2006).
- [16] D. Cao, F. Bridges, G. R. Kowach, and A. P. Ramirez, Phys. Rev. Lett. **89**, 215902 (2002).
- [17] N. L. Ross, J. Zhao, and R. J. Angel, J. Solid state Chem. **177**, 3768 (2004).
- [18] J. Rouquette, J. Haines, V. Bornand, M. Pintard, Ph. Papet, W. G. Marshall, and S. Hull, Phys. Rev. B **71**, 024112 (2005).